Journal of Hydroscience and Hydraulic Engineering
Vol. 1, No. 1, April, 1983, pp.53-63.

STABILITY AND VERTICAL MIXING PROCESS IN DOUBLE-DIFFUSIVE STRATIFICATION SYSTEM COMPOSED OF HEAT-SALT COMPLEX

By

Akira Murota

Department of Civil Engineering, Osaka University, Suita, Osaka, Japan

and

Kohji Michioku

Department of Civil Engineering, Osaka University, Suita, Osaka, Japan

SYNOPSIS

The stability and the vertical mixing process in an double-diffusive stratification system composed of heat-salt complex in which a stable gradient of salt concentration is heated at the bottom of the container are investigated, experimentally and theoretically. Using the variational principle, a stability analysis for the system with arbitrary distribution profiles of two density components is presented. The theoretical solutions are applicable to any possible distribution profiles of two components. Applying the theory to the system with heat-salt complex, we have satisfactory agreement between the theoretical and experimental results. At the initial stage of the instability, a sharp interface of stratification is formed at a finite depth below which the fluid is uniformly mixed. To simply discuss the convection process at the double-diffusive interface, an experiment in which a fresh-salt two-layer system is heated at the bottom of the container is conducted. As the density interface becomes unstable due to the negative thermal buoyancy, the interfacial fluctuations are generated and turbulent lumps of buoyant fluid are increasingly entrained across the interface. This means that both heat and solute flux is composed of both the advective entrainment and the molecular diffusion. These two types of transportation are confirmed quantitatively by evaluating individually the conductive and convective components of the heat flux across the interface. The interfacial fluctuations observed in this experiment have some similar characteristics to those of the Linden's experiment of the vortex ring (4). Finally, it is verified that the entrainment coefficient and Richardson number has the well-known functional form, $E \propto R_i^{-1 \sim -3/2}$, which is reported by some researchers in the experiments of the deepening process induced by the mechanical energy.

INTRODUCTION

In the thermal stratification field in the closed water mass, such as lakes and reservoirs, the heat transport process being originated by heat supply or release at the water surface and horizontal intrusion of water mass with a different temperature or turbidity may result some local instability of temperature gradient and this will behave as the trigger of the thermal convection. This process may lead to the deepening of the epilimnion(the surface mixing layer) and the vertical transport of solute and suspended solids in a stratified field. Thus, to examine the stability criterion and the vertical transport process induced by the heat convection is practically important for the evaluation of the water qualities.

In general, if both heat and solute contribute to establish the density gradient of field, the resulting thermosolutal convection essentially differs from

the single thermal convection because of the different diffusion rate of each component . This specific convection is generally called the double-diffusive phenomena and two different states are classified(15). One is the state in which the density component with larger diffusivity has a stable density gradient and other component with smaller diffusivity has an unstable gradient. This system is called " a double-diffusive stratification system in finger régime " and , for example, in the heat-salt complex system, this régime corresponds to the case in which the thermal density gradient is gravitationally stable and the salt concentration gradient is unstable. On the other hand, the contrary case with a stable salt gradient and an unstable temperature gradient is called " a double-diffusive stratification system in diffusive régime " . As the vertical mixing process induced by the thermal convection is in the diffusive régime, the authors will focus their attention on the latter case and investigate the stability and the mixing process.

Veronis (17) and Stern (11) analyse the critical condition on the initiation of convection for the simple case where both of two density components have constant gradients. Tamai et al. (16) examine the stability of the practical system with parabolic distribution profile of one component and linear one of another component. On the other hand, the stability analysis in this paper gives more general criterion which is applicable to any possible distribution profiles of two components. The result is compared with the experiment performed in the heat-salt complex system in which a initially stable salinity gradient is heated at the bottom of the container.

After the onset of the instability, the fluid below a finite height begins to mix and a sharp density interface is established. To discuss the convective transport process at the interface, the behavior of a two-layer heat-salt system is experimentally investigated in the third chapter. Turner (12), Crapper (1), Linden (5) and so on, have carried out similar experiments and have succeeded in clarifying some aspects of this process. The original results of our experiment are as follows:

1) The influence of advective entrainment process across the interface on the mass transport is understood in more detail.
2) The correlation between the interfacial fluctuation properties and the heat flux has been verified.
3) The entrainment coefficient is evaluated by means of the convecting velocity scale and it is related with Richardson number.

STABILITY OF THE DOUBLE-DIFFUSIVE STRATIFICATION SYSTEM

The stability to infinitesimal disturbances of a double-diffusive stratification system shown in Fig.1(a) is preliminary investigated(8). $T_0^*(z^*)$ and $S_0^*(z^*)$ are

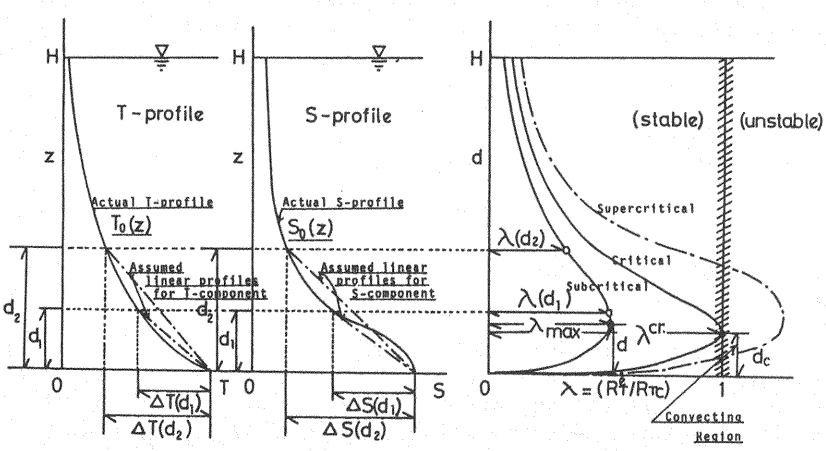

Fig. 1 Schematic diagrams of the distribution profiles of two components and illustration of the stability parameter λ and the range d

the mean concentration of components with higher and lower diffusivities, respectively. The linearized momentum and continuity equations can be written as follows:

$$-\frac{\partial V^*}{\partial t^*} = -\frac{1}{\rho_0^*}\,\mathrm{grad}.p^* - \frac{\rho^*}{\rho_0^*}\,g\cdot k + \nu\nabla^{*2}V^* \tag{1}$$

$$\nabla^* V^* = 0 \tag{2}$$

where $V^* = (u^*,v^*,w^*)$ = vector flow velocity; g = gravity acceleration; ρ^* = density of the fluid; ν = kinematic viscosity, ∇^* = vector operator; and k = unit vector in the z^* direction. The linearized equation of state is

$$\rho^* = \rho_0^*\,[\,1 - \alpha(T_0^*(z^*) + T^*) + \beta(S_0^*(z^*) + S^*)\,] \tag{3}$$

where T^*, S^* = contributions for two components due to convection; α , β = corresponding coefficients of expansion defined as $\alpha = -(1/\rho_0^*)\cdot(\partial\rho^*/\partial T^*)$, $\beta = (1/\rho_0^*)\cdot(\partial\rho^*/\partial S^*)$. The equations for the conservation of T^* and S^* properties are

$$\frac{\partial}{\partial t^*}\begin{pmatrix}T^*\\S^*\end{pmatrix} + w^*\frac{d}{dz^*}\begin{pmatrix}T_0^*\\S_0^*\end{pmatrix} = \begin{pmatrix}\kappa_T\nabla^{*2}T^*\\\kappa_S\nabla^{*2}S^*\end{pmatrix} \tag{4}$$

where κ_T, κ_S = molecular diffusivities ($\kappa_S \leq \kappa_T$).

The boundary conditions on the upper and lower ends are represented by

$$w^* = 0\ ;\ \frac{\partial^2 w^*}{\partial z^{*2}} = 0\ ;\ T^* = S^* = 0 \quad \text{for} \quad z^* = 0 \text{ and } d\ . \tag{5}$$

The infinitesimal purturbations for w^* , T^* and S^* may have the following forms.

$$\begin{pmatrix}w^*\\T^*\\S^*\end{pmatrix} = \begin{pmatrix}W^*(z^*)\\T^*(z^*)\\S^*(z^*)\end{pmatrix}\exp.[\,i\,(a_x^*x^* + a_y^*y^*) + (\sigma_r^* + i\sigma_m^*)t^*\,] \tag{6}$$

Eliminating u^*, v^*, p^* and ρ^* in Eqs. 1-4 and substituting Eq. 6 into them, we obtain a set of equations for W^*, T^* and S^*. Now, we apply the variational principle introduced by Nield (9). Multiplying these equations by W^*, T^* and S^*, respectively and integrating them over the range of z^*, we have

$$\langle(D^2W) + 2a^2(DW)^2 + a^4W^2)\rangle + \sigma\langle(DW)^2 + a^2W^2\rangle - R_T^{\frac{1}{2}}\,a\langle WT\rangle + R_S^{\frac{1}{2}}\,a\langle WS\rangle = 0 \tag{7}$$

$$-\langle(DT)^2 + a^2T^2\rangle + R_T^{\frac{1}{2}}\,a\langle WTf(z)\rangle - P_r\sigma\langle T^2\rangle = 0 \tag{8}$$

$$-\langle(DS)^2 + a^2S^2\rangle + \frac{1}{\tau}R_S^{\frac{1}{2}}\,a\langle WSg(z)\rangle - \frac{P_r\sigma}{\tau}\langle S^2\rangle = 0 \tag{9}$$

where we use the non-dimensional expressions for each term as follows:

$$t^*=t(d^2/\nu);\ z^*=zd;\ W^*=\pi_1 W;\ T^*=\pi_2 T;\ S^*=\pi_3 S;$$

$$\frac{\pi_2}{\pi_1} = \sqrt{\frac{\Delta T\nu}{\alpha g a^{*2}d\kappa_T}}\ ;\ \frac{\pi_3}{\pi_1} = \sqrt{\frac{\Delta S\nu}{\beta g a^{*2}d\kappa_T}}\ ;\ a^* = \sqrt{a_x^{*2} + a_y^{*2}}\ ;$$

$$R_T=\alpha g\Delta T d^3/\kappa_T\nu\ ;\ R_S=\beta g\Delta S d^3/\kappa_T\nu\ ;\ \tau=\kappa_S/\kappa_T\ ;\ P_r=\nu/\kappa_T\ ;$$

$$f(z)=-(d/\Delta T)(dT_0^*/dz^*)\ ;\ g(z)=-(d/\Delta S)(dS_0^*/dz^*)$$

and angular brackets in Eqs. 7~9 denote integrations over the range $0 \leq z \leq 1$.

Now let's put

$$W = C_1 W_1 \quad ; \quad T = C_2 T_1 \quad ; \quad S = C_3 S_1 \tag{10}$$

where W_1, T_1 and S_1 are suitably chosen trial functions. Substituting Eq. 10 into Eqs. 7~9 and eliminating C_1, C_2 and C_3 and dropping the subscripts, we can get the following characteristic equation.

$$R_T a^2 \frac{\langle WT \rangle \langle WTf(z) \rangle}{\langle (DT)^2 + a^2 T^2 + P_r \sigma T^2 \rangle} - \frac{1}{\tau} R_S a^2 \frac{\langle WS \rangle \langle WSg(z) \rangle}{\langle (DS)^2 + a^2 S^2 + P_r \sigma S^2/\tau \rangle}$$

$$= \langle (D^2 W)^2 + 2a^2 (DW)^2 + a^4 W^2 \rangle + \sigma \langle (DW)^2 + a^2 W^2 \rangle \tag{11}$$

The above equation is a cubic in σ and it can be rewritten as follows

$$a_1 \sigma^3 + a_2 \sigma^2 + a_3 \sigma + a_4 = 0 \tag{12}$$

where $\sigma = \sigma_r + \sigma_m i$.
Because the critical condition for the marginal stability is $\sigma_r = 0$, we can substitute $\sigma = \sigma_m i$ into Eq. 12.

Now, we consider two cases of instability. First, when a direct mode instability with no oscillations occurs, ie. $\sigma_m = 0$, the criterion is defined as

$$a_4 = 0 \tag{13}$$

Secondly, in the case of the oscillatory mode instability, ie. $\sigma_m \neq 0$, we derive two equations from Eq. 12 by seperately equating to zero the real and imaginary parts of the equation. Eliminating the term σ_m in them, we obtain

$$a_1 a_4 - a_2 a_3 = 0 \tag{14}$$

as the criterion. If we choose $W_1 = T_1 = S_1 = \sin \pi z$ as the trial functions satisfying the boundary conditions, Eqs. 13 and 14 have the following forms.

$$R_T = \frac{\langle \sin^2 \pi z \cdot g(z) \rangle R_S}{\langle \sin^2 \pi z \cdot f(z) \rangle \tau} + \frac{(\pi^2 + a^2)^3}{2 \langle \sin^2 \pi z \cdot f(z) \rangle a^2} \tag{15}$$

$$R_T = \frac{(1 + \tau/P_r) \langle \sin^2 \pi z \cdot g(z) \rangle}{(1 + 1/P_r) \langle \sin^2 \pi z \cdot f(z) \rangle} R_S + \frac{(P_r + \tau)(\tau + 1)}{P_r} \cdot \frac{(\pi^2 + a^2)^3}{2a^2 \langle \sin^2 \pi z \cdot f(z) \rangle} \tag{16}$$

The critical Rayleigh number for the onset of instability in each case is, therefore, determined by the condition

$$\frac{\partial R_T}{\partial a^2} = 0 \quad \text{or} \quad a^2 = \pi^2/2 \quad \text{(the most unstable wave number)} \tag{17}$$

which is equal to the condition for linear profiles of two components. For the above condition , the critical condition for two cases are deduced as follows

$$R_{Tc} = \frac{\langle \sin^2 \pi z \cdot g(z) \rangle R_S}{\langle \sin^2 \pi z \cdot f(z) \rangle \tau} + \frac{27\pi^4}{8 \langle \sin^2 \pi z \cdot f(z) \rangle} \quad \text{(direct mode)} \tag{18}$$

$$R_{Tc} = \frac{(1 + \tau/P_r) \langle \sin^2 \pi z \cdot g(z) \rangle}{(1 + 1/P_r) \langle \sin^2 \pi z \cdot f(z) \rangle} \cdot R_S + \frac{(P_r + \tau)(\tau + 1)}{P_r} \cdot \frac{27\pi^4}{8 \langle \sin^2 \pi z \cdot f(z) \rangle} \tag{19}$$

(oscillatory mode)

where R_{Tc} is the critical Rayleigh number for T-component. With the linear distribution of T- and S-components, ie. $f(z) = g(z) = 1$, Eqs. 18 and 19 coincide with the solutions obtained by Stern (11) and Veronis(17) , respectively. In addition, in

the case of the pure thermal convection, ie. $R_S=0$, Eq. 18 agrees with the Nield's result (19).

As we mainly examine the oscillatory mode instability in this paper, particularly Eq. 19 is compared with the experiment. To evaluate the influence of distribution profiles of concentration on the stability criterion, the experiment is performed in a heat-salt system in which salinity stratifications with various types of initial salinity distribution profiles are heated at the bottom of the container. Detailed descriptions on the experimental equipments will be given later.

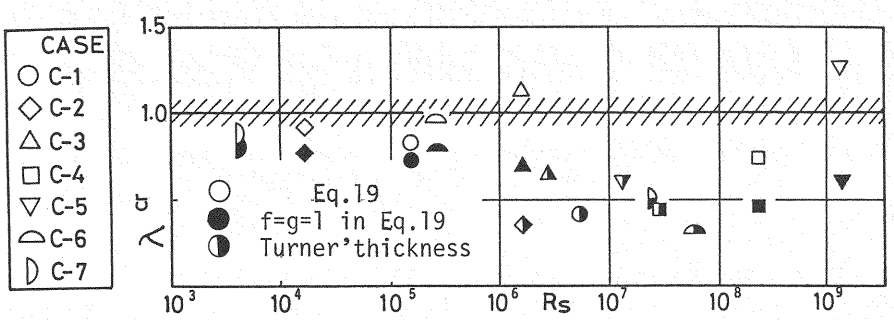

Fig. 2 Critical values of λ against the salinity Rayleigh number R_S

The open symbols in Fig. 2 denote the ratio of the experimental critical Rayleigh number to the theoretical one given by Eq. 19 , $\lambda^{cr}=(R_S^c/R_{Tc})^{cr}$, as a function of the salinity Rayleigh number R_S^c, where the height at which λ^{cr} takes the maximum value is used as the length scale d (see Fig. 1(b)). For comparison, λ^{cr} values in the case where R_{Tc} is computed assuming constant temperature and salinity gradients between the bottom and the top of the depth d, ie. $f(z)=g(z)=1$, in Eq. 19 (see the chain lines in Fig. 1(a)), are also shown by the solid symbols. The semi-open symbols represent the values in which the thermal sublayer thickness proposed by Turner (13) is used as the length scale d. As the open symbols agree better with unity than others, the stability criterion computed from Eq. 19 must be most reasonable. Consequently, it is concluded that the effect of the distribution profiles of two components should be taken into consideration when we evaluate the stability criterion in a double-diffusive stratification.

VERTICAL MIXING PROCESS OF THE TWO-LAYER SYSTEM

When the convective motion begins, a sharp density interface are formed and temperature and solute are transported across the interface by the convective motion, In this chapter, the vertical mixing process in a two-layer system is treated experimentally for a simple case of the thermosolutal convection.

Experimental equipments

The experiments are performed by using a small plastic container (20cm long, 8cm wide and 40cm deep). Heat is supplied uniformly over the bottom of the container by means of a rubber heater. The experimental conditions are presented in Table 1 , where h_1 and h_2 are the initial upper and lower layer thickness , respectively and S_2 the initial salinity concentration of the lower layer. The upper layer is composed with the fresh water. The measurements of temperature and salinity are made by using some thermistor probes and an electorode conductivity probe. Visual observations of the mixing process are carried out by the video camera system.

Table 1
Experimental condition

CASE	h_2 (cm)	h_1 (cm)	S_2 (%)	F_{To} (cm°C/s)	Symbols
TL1	5.1	14.9	0.453	0.0567	○
TL2	7.5	12.5	0.473	0.0528	◑
TL3	9.9	10.1	0.461	0.0564	⊕
TL4	12.6	7.4	0.500	0.0525	◑
TL5	15.1	4.9	0.427	0.0567	●
TL6	5.0	15.0	0.217	0.0508	◇
TL7	7.5	12.5	0.307	0.0513	◈
TL8	10.0	10.0	0.227	0.0575	◈
TL9	15.1	4.9	0.246	0.0568	◆

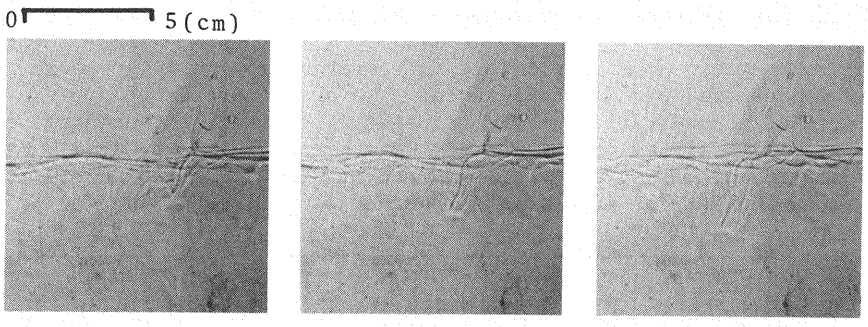

Photo. 1 Visual observation of entrainment process at a two-layer interface (time interval is 0.8(sec))

Characteristics of interfacial fluctuation

At the early stage after the heating starts, the predominant stability effects of the solute density gradient inhibits the convective heat transfer across the interface, thus, both heat and solute may be transported only by the molecular diffusion. As the net density difference decreases with time owing to the heat supply and the interface becomes gravitationally unstable, fluctuations are generated at the interface. This may be the same phenomena as the interfacial domes observed in the experiment of the penetrative convection reported by Denton et al. (2). With increasing of the level of the displacement of interface, the vertical transports of turbulent patches across the interface become more violent. The entrainment process of buoyant fluid elements is shown in Photo. 1. This advective entrainment makes the interface migrate upward by the expense of the upper layer as shown in Fig. 3. In the final stage, as the effective density anomaly approaches to zero, the fluctuation grows up within the overall domain of the field and fluid are completely overturned.

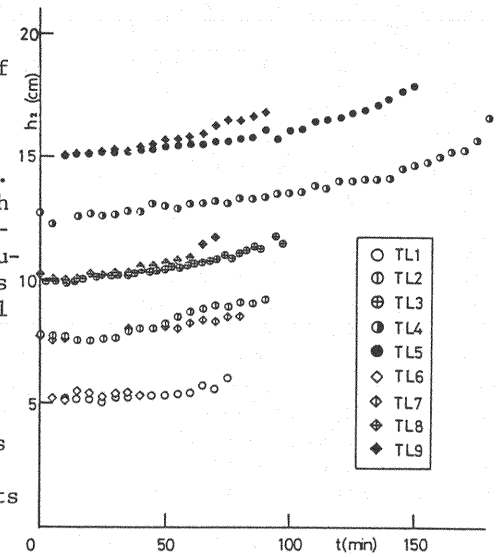

Fig. 3 Changes of the lower layer depth

Fig. 4 shows the relationship between the normalized height of the interfacial fluctuation H/h_2 and the density ratio $R_\rho=\Delta\rho_S/\Delta\rho_T$, where H is the maximum height of the interfacial waves during about one minute, $\Delta\rho_T$ and $\Delta\rho_S$ the thermal and solute density difference between two layers, respectively. In this figure, it is noteworthy that H/h_2 increases rapidly with R_ρ decreasing from about 2.8(6), which implies that the entrainment of the buoyant fluid may also increase below around $R_\rho=2.8$. A similar tendency is reported by Ozaki et al. (10).

As the interfacial domes may be generated by the impact of the thermal

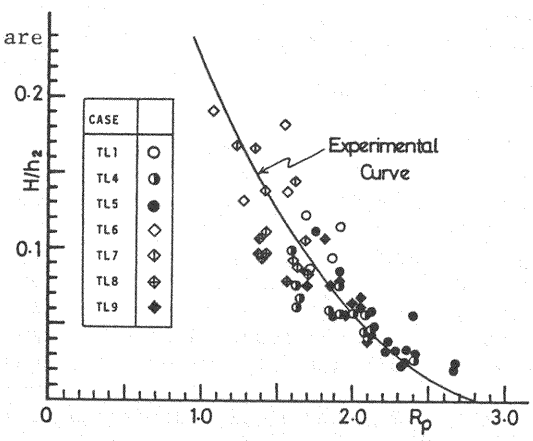

Fig. 4 Non-dimensional displacement H/h_2 versus stability R_ρ

plumes, it is significant to compare our results with Linden's experiment (4) in which he measures the interfacial distortion produced by the impact of the falling vortex ring. Linden's data are modified on the following assumptions.

i) The penetration depth of the vortex ring is about half times of H.
ii) The falling velocity of the vortex ring is equivalent to the convective velocity.
iii) The vortex ring diameter is equivalent to the length scale of the convective motion which equal to about $0.1h_2$. (2)

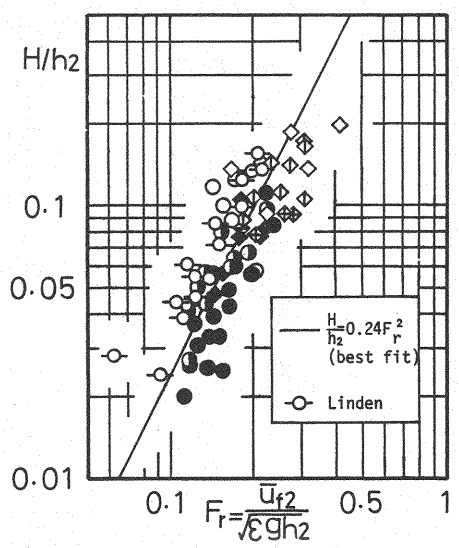

Fig. 5 H/h_2 versus densimetric Froude number F_r

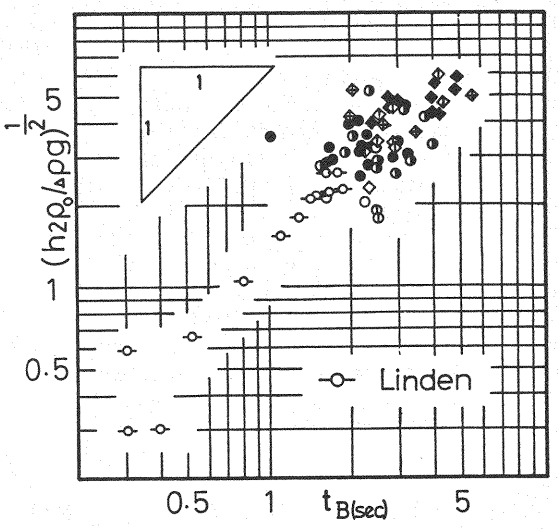

Fig. 6 Time scale t_B for the recoil of the interface versus Brunt-Väisälä time.

Fig. 5 shows the relationship between H/h_2 and the densimetric Froude number $F_r=\bar{u}_{f2}/\sqrt{\varepsilon g h_2}$, where $\bar{u}_{f2}$ is the convecting velocity scale of the lower layer discussed later. The functional form, $H/h_2 \propto F_r^2$, coincides with Linden's theoretical model for the vortex ring. In Fig. 6, the time scale t_B for the recoil of the interface is plotted against Brunt-Väisälä time. Both data of author's and Linden's are proportional to Brunt-Väisälä time, which implies that the interfacial penetration recoils in the way of the gravity wave. These results suggest that the interfacial fluctuation in this experiment is generated in the same manner as that in the vortex ring experiment.

Heat flux across the density interface

Based on the consideration in the previous section, it may be of reasonable modelling that the total flux across the interface is composed of the entrainment and the diffusive components (5). In addition, we assume that the entrainment velocity is composed of such two components as the upward velocity U_e^U and the downward one U_e^L and that the interface migration is caused by the unbalance between them (7). Applying these models to a system in Fig.7, the conservation of heat, salt and volume leads to a following set of equations.

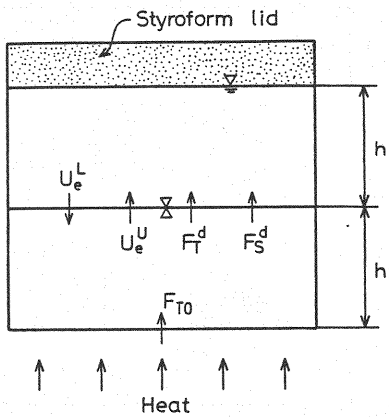

Fig. 7 Conservation in the ideal two-layer system

h_1, h_2 ; lower and upper layer depth

F_{T0} ; heat flux at the bottom

$$\frac{d}{dt}\begin{pmatrix} h_i T_i \\ h_i S_i \\ h_i \end{pmatrix} = \begin{cases} (U_e^u T_2 - U_e^L T_1 + F_T^d)\xi_i + F_{T_0}\delta_{i2} \\ (U_e^u S_2 - U_e^L S_1 + F_S)\xi_i \\ (U_e^u - U_e^L)\xi_i \end{cases} = \begin{pmatrix} F_T\xi_i + F_{T_0}\delta_{i2} \\ F_S\xi_i \\ (U_e^u - U_e^L)\xi_i \end{pmatrix} \qquad (20)$$

$$\xi_i = \begin{cases} 1 & (i=1) \\ -1 & (i=2) \end{cases} \qquad \delta_{i2} = \begin{cases} 0 & (i=1) \\ 1 & (i=2) \end{cases}$$

Where F_{T0}= heat flux at the bottom of the container; and F_T^d, F_S^d = diffusive components of heat and salt flux, respectively. From measurement of the time histories of temperature, salinity and depth of each layer, U_e^u, U_e^L, F_T^d and F_S^d can be calculated from Eq. 20. In this calculation, the theoretical value for the ratio, $\beta F_S^d/\alpha F_T^d = \sqrt{\kappa_S/\kappa_T}$ (9), is introduced.

The total heat flux F_T, the entrainment heat flux $F_T^e = U_e^u T_2 - U_e^L T_1$ and the diffusive heat Flux F_T^d are shown as a function of R_ρ in Fig. 8, 9 and 10, respectively. They are normalized on F_{Tp} which is the theoretical heat flux between two solid planes with the same temperature difference at the interface. The solid lines indicate the best fit curves of the data points.

For comparison, the experimental curves of Turner's (13) and Crapper's (1) are also plotted in Fig. 9. Because Turner does not allow for changes in the layer volumes in his calculation of the heat flux, his experimental values are greater than Author's and Crapper's . Judging from this results, the importance of the advective entrainment process in the estimation of the thermosolutal flux should be emphasized.

As may be seen from Fig. 9, the entrainment flux increases rapidly below around R_ρ=2.8, which is much consistent with Fig. 4. Therefore, it is concluded that the weakened interfacial constraints

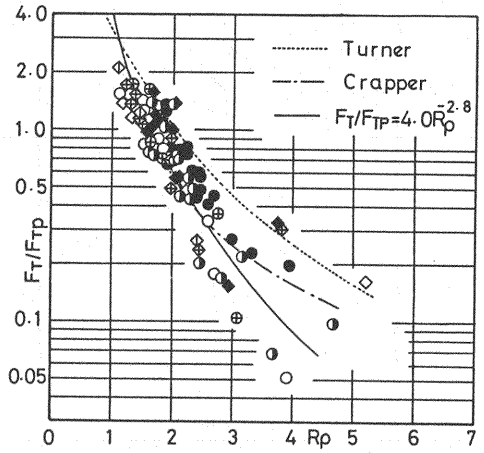

Fig. 8 Non-dimensional total heat flux F_T/F_{Tp} versus R_ρ

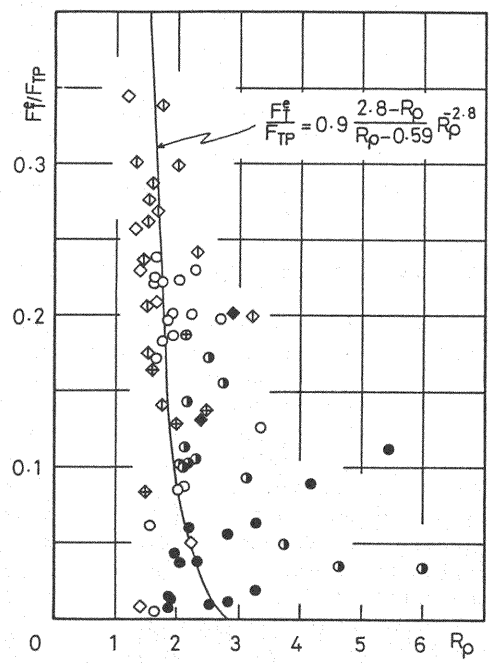

Fig. 9 Non-dimensional entrainment component of the heat flux F_T^e/F_{Tp} against R_ρ

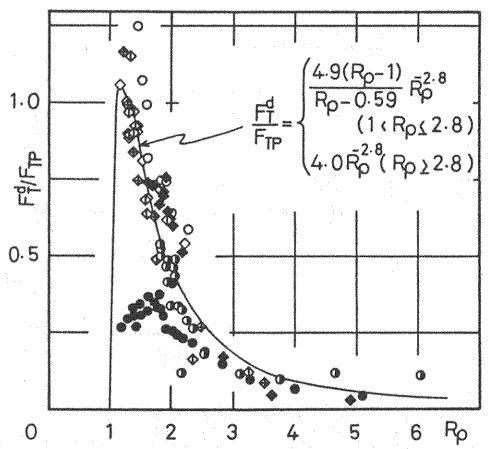

Fig. 10 Non-dimensional diffusive component of the heat flux F_T^d/F_{Tp} against R_ρ

due to the decrease of R_ρ can allow to distort the interface and to break away fluid elements, and that the entrainment is promoted by the intense of fluctuations at the interface.

Although the diffusive flux F_T^d must theoretically approach to zero as R_ρ decrease to unity, the data nearby R_ρ=1 cannot be obtained because of the observational error, as seen in Fig. 10.

Evaluation of the entrainment coefficient

In this section, we estimate the velocity scale of the convecting layer using a simple model and evaluate the entrainment coefficient as a function of Richardson number.

As we can neglect the diffusion effect in the convecting layer, the equation for the conservation of heat is written as,

$$\partial T_i/\partial t = -\partial/\partial z\cdot(u_{fi}T') \qquad (i=1,2) \tag{21}$$

where u_{fi} = horizontally averaged velocity of the thermal plumes; T'= contribution for temperature to convection. As the mean temperature is nearly uniform throughout the convecting layer, we can put $\partial T_i/\partial t=dT_i/dt$. Integrating Eq. 21 under the boundary conditions

$$u_{f2}T'= F_{T_0} \ (z=-h_2) \ ; \ u_{f1}T'= u_{f2}T'= F_T \ (z=0) \ ; \ u_{f1}T'= 0 \ (z=h_1) \tag{22}$$

the convecting heat flux $u_{fi}T'$ is obtained as

$$u_{f1}T'= F_T(h_1 - z)/h_1 \ ; \ u_{f2}T'= (F_T - F_{T0})(z + h_2)/h_2 + F_{T0} \tag{23}$$

The solute flux is also caluculated by the same procedure as

$$u_{f1}S'= F_S(h_i - z)/h_1 \ ; \ u_{f2}S'= F_S(z + h_2)/h_2 \tag{24}$$

Next, we assume that the potential energy of the buoyant fluid $\rho_0(\alpha T'-\beta S')g\delta z$ is transformed to the kinetic energy $\delta(1/2\cdot\rho u_{fi}^2)$ along the small distance δz. Then, the energy balance is written as,

$$\frac{1}{2}d(u_{fi}^2) = (\alpha T'- \beta S')g\cdot dz \tag{25}$$

Eliminating T'and S'in Eqs. 23-25, we obtain u_{fi} (i=1,2). Integrating them within each layer, the mean convecting velocity scale are obtained as

$$\overline{u}_{f1} = \left\{(\alpha F_T + \frac{\alpha F_T - \beta F_S}{2})gh_1\right\}^{\frac{1}{3}} \ ; \ \overline{u}_{f2} = \left\{(\alpha F_T - \beta F_S)gh_2\right\}^{\frac{1}{3}} \tag{26}$$

Assuming that the upward and downward entrainment are caused by the turbulent motion in the upper and lower layer, respectively, we define the entrainment coefficient and Richardson number for each layer as follows

$$E^u=U_e^u/\overline{u}_{f1} \ ; \ E^L=U_e^L/\overline{u}_{f2} \ ; \ R_i^u=\varepsilon gh_1/\overline{u}_{f1}^2 \ ; \ R_i^L=\varepsilon gh_2/\overline{u}_{f2}^2 \tag{27}$$

The relationship between E and R_i for each layer is shown in Fig. 11. It is interesting that, in the figure, their relationships have the well-known functional form as, $E^{u(L)} \propto R_i^{u(L)\ -1\sim-3/2}$. It suggests that, even in the double-diffusive stratification system, the mechanism of the convective transport across the interface may be essentially equivalent to that produced by the mechanical energy such as the vortex ring, the mechanical stirring grid (14) and the stratified shear flow (3). As a result, it is concluded that, if we evaluate the velocity and the length scale reasonably, we can estimate the entrainment component of the vertical mixing flux.

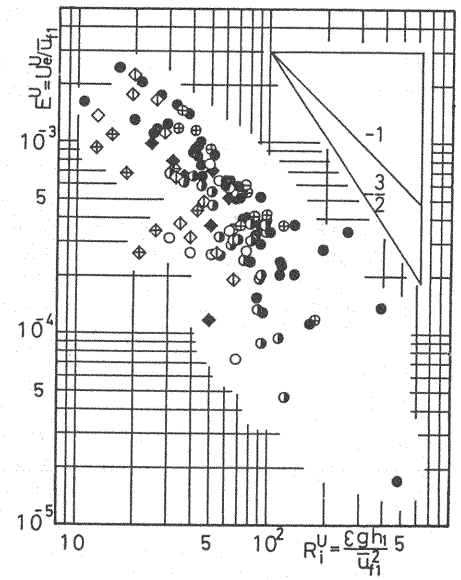

(a) Upward entrainment coefficient $E^u=U_e^u/\overline{u}_{f1}$ versus Richardson number $R_i^u=\varepsilon g h_1/\overline{u}_{f1}^2$

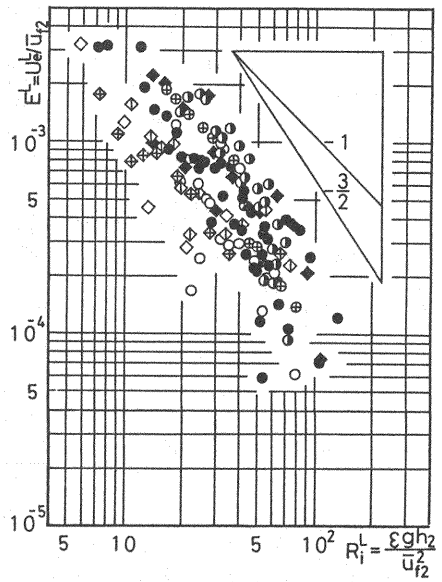

(b) Downward entrainment coefficient $EL=U_e^L/\overline{u}_{f_2}$ versus Richardson number $R_i^L=\varepsilon g h_2/\overline{u}_{f2}^2$

Fig. 11 Entrainment coefficient as a function of Richardson number

SUMMARY

The stability and the mixing process in the stratification system of heat-salt complex are studied. The results are summarized as follows.

A stability analysis for the system with arbitrary distribution profiles of two density components is developed and their results are in agreement with the experimental ones. As a conclusion, it would be important to take into account the effect of the distribution profiles of temperature and salinity concentration to examine the stability criterion.

In a two-layer system, in which the salinity stratification is heated at the bottom of the container, the fluctuation at the interface has some similar characteristics to the experimental results of the vortex ring. Next, using the equation of the conservation for heat, salt and volume in a two-layer system, the upward and downward velocity of the entrainment and the diffusive heat flux are seperately evaluated. They are related with the stability at the interface. It is clarified that the entrainment heat flux shows an important role in the mixing process in the double-diffusive stratification system and that it is closely related with the level of the interfacial fluctuation. In addition, the entrainment coefficient E decreases as Richardson number R_i increases with the well-known functional form, $E \propto R_i^{-1 \sim -3/2}$. These results show that the mechanism of the interfacial entrainment produced by the heat convection is much analogous to that of the deepening process performed with some mechanical stirring, eg. the vortex ring, the stirring grid and the stratified shear flow.

REFERENCES

1. Crapper, P.F. : Measurement across a diffusive interface, Deep-Sea Research, Vol.22, pp.537-545, 1975.
2. Denton, R.A. and I.R. Wood : Penetrative convection at low Péclet number, Journal of Fluid Mechanics, Vol.113, pp.1-21, 1981.
3. (for example) Kato, H. and O.M. Phillips : On the penetration of turbulent layer into stratified fluid, Journal of Fluid Mechanics, Vol.37, pp.643-655, 1969.
4. Linden, P.F. : The interaction of a vortex ring with a sharp density interface : a model for turbulent entrainment, Journal of Fluid Mechanics, Vol.60, pp.467-480, 1973.
5. Linden, P.F. : A note on the transport process across a diffusive interface, Deep-Sea Research, Vol.21, pp.283-287, 1974.
6. Murota, A. and K. Michioku : Stability and vertical mixing of a two-layer density stratification heated at the bottom, Technology Reports of Osaka University, Vol.32, pp.391-399, 1982.
7. Murota, A. and K. Michioku : Study on vertical mixing of stratified fluid in diffusive résime Proceeding of 26th Japanese Conference on Hydraulics, pp.391-399, 1982(in Japanese).
8. Murota, A. and K. Michioku : Effects of temperature and salinity profiles on stability criterion in double-diffusive stratification, Technology Reports of Osaka University, Vol.33, 1983(in print).
9. Nield, D.A. : The onset of transient convective instability, Journal of Fluid Mechanics, Vol.71, pp.441-454, 1975.
10. Ozaki, H., T. Asaeda and N. Tamai : Proceeding of 36th Annual Conference of JSCE, pp.407-408, 1982(in Japanese).
11. Stern, M.E. : The "salt-fountain" and thermohaline convection, Tellus, Vol.12, pp.172-175, 1960.
12. Turner, J.S. : The coupled turbulent transports of salt and heat across a sharp density interface, International Journal of Heat and Mass Transfer, Vol.8, pp.759-767, 1965.
13. Turner, J.S. : The behavior of a stable salinity gradient heated from below, Journal of Fluid Mechanics, Vol.33, pp.183-200, 1968.
14. (for example) Turner, J.S. : The influence of molecular diffusivity on turbulent entrainment across a density interface, Journal of Fluid Mechanics, Vol.33, pp.639-656, 1968.
15. Turner, J.S. : Double-diffusive phenomena, Annual Review of Fluid Mechanics, Vol.6, pp.37-56, 1974.
16. Tamai, N., T. Asaeda and Y. Takahashi : Stability and development of mixed layers in heat-salt double-diffusive process, Proceeding of 24th Japanese Conference on Hydraulics, pp.429-434, 1980.
17. Veronis, G. : On finite amplitude instability in thermohaline convection, Vol.23, pp.1-17, 1965.